Korean Chem. Eng. Res., 59(4), 493-502 (2021)
https://doi.org/10.9713/kcer.2021.59.4.493
PISSN 0304-128X, EISSN 2233-9558

Kinetics, Isotherm and Adsorption Mechanism Studies of Letrozole Loaded Modified and Biosynthesized Silver Nanoparticles as a Drug Delivery System: Comparison of Nonlinear and Linear Analysis

Mahsa PourShaban*, Elham Moniri, Raheleh Safaeijavan***† and Homayon Ahmad Panahi******

**Department of Biotechnology, Science and research Branch, Islamic Azad University, Tehran, Iran*
***Department of Chemistry, Varamin-Pishva Branch, Islamic Azad University, Varamin, Iran*
****Department of Biochemistry and Biophysics, Varamin-Pishva Branch, Islamic Azad University, Varamin, Iran*
*****Department of Chemistry, Central Tehran Branch, Islamic Azad University, Tehran, Iran*
(Received 8 January 2021; Received in revised from 26 May 2021; Accepted 5 August 2021)

Abstract – We prepared and investigated a biosynthesized nanoparticulate system with high adsorption and release capacity of letrozole. Silver nanoparticles (AgNPs) were biosynthesized using olive leaf extract. Cysteine was capped AgNPs to increase the adsorption capacity and suitable interaction between nanoparticles and drug. Morphology and size of nanoparticles were confirmed using transmission electron microscopy (TEM). Nanoparticles were spherical with an average diameter of less than 100 nm. Cysteine capping was successfully confirmed by Fourier transform infrared resonance (FTIR) spectroscopy and elemental analysis (CHN). Also, the factors of letrozole adsorption were optimized and the linear and non-linear forms of isotherms and kinetics were studied. Confirmation of the adsorption data of letrozole by cysteine capped nanoparticles in the Langmuir isotherm model indicated the homogeneous binding site of modified nanoparticles surface. Furthermore, the adsorption rate was kinetically adjusted to the pseudo-second-order model, and a high adsorption rate was observed, indicating that cysteine coated nanoparticles are a promising adsorbent for letrozole delivery. Finally, the kinetic release profile of letrozole loaded modified nanoparticles in simulated gastric and intestinal buffers was studied. Nearly 40% of letrozole was released in simulated gastric fluid with pH 1.2, in 30 min and the rest of it (60%) was released in simulated intestinal fluid with pH 7.4 in 10 h. These results indicate the efficiency of the cysteine capped AgNPs for adsorption and release of drug letrozole for breast cancer therapy.

Key words: Silver nanoparticles, Cysteine, Drug delivery, Letrozole, Non-linear and linear

1. Introduction

Nanotechnology is a multidisciplinary science that deals with particles in size 10-100 nm. At the nano size, molecules work differently, which makes it possible for scientists to focus on it in various fields such as medicine, pharmacy [1]. Using functionalized surface coatings, nanoparticles are able to contribute to the conjugation of chemotherapeutic drugs or employ target ligands to enhance their usefulness for targeted therapy and drug delivery [2].

Among different metal nanoparticles, AgNPs have attracted a great deal of attention due to their biomedical applications [3]. The toxic effects of Ag NPs should be studied properly because the numerous usage areas of these NPs such as water purification systems [4], pharmaceutical applications [5], food packaging processes and textile industry [6] make them as an outstanding material for the environment and humankind. Nowadays, only a few studies have studied the possible toxic effects of orally administered AgNPs [7-10].

A variety of methods are used to synthesize AgNPs, such as physical, biological and chemical. Since physico-chemical methods are costly or require toxic substances, they are not among the preferred synthesis methods [11]. Among biosynthetic methods, plant materials are particularly used for nanoparticles synthesis mainly because they obviate the need for complex procedures such as intracellular synthesis and manifold purification steps [12].

Olive leaf extract includes compounds that display powerful antimicrobial activities against fungi, bacteria and mycoplasma. The primarily active components of the olive leaf are Oleuropein and its derivatives including tyrosol and hydroxyl tyrosol [13].

Chemotherapeutic drugs do not have any specificity towards tumor site, which is the main problem for cancer therapy as they affect both cancerous and normal cells. So, large doses of drugs with perilous side effects have to be injected to reach efficient local concentrations at the tumor. Then, researchers seek to develop targeted drug delivery strategies such as magnetic and molecular targeting systems [2].

Nanoparticles use both passive and active targeting strategies to increase the intracellular concentration of drug in cancer cells without causing toxicity in normal cells [14,15]. The appropriate surface functionalization of nanoparticles is a perquisite of any feasible applications that determine how they interact with the environment. These interactions ultimately influence nanoparticles stability, leading to a controlled assembly or nanoparticles delivery to a target, for

† To whom correspondence should be addressed.
E-mail: moniri30003000@yahoo.com, safaeijavan@gmail.com

instance, by applying suitable functional molecules to the particle surface. Among the capped/coated AgNPs, increasing attention has been allocated to cysteine capped AgNPs due to their distinctive sensing and biological activities towards amino acids and microorganisms [16].

The drug release from pharmaceutical nanoparticles is a major determinant of its biological effects, so evaluation of drug release kinetic is very important in this field. The kinetic model is often helpful to illustrate release mechanisms [17]. A fairly potent and selective aromatase inhibitor, letrozole hampers enzyme activity in patients that suffer from advanced breast cancer. Letrozole has been shown to be more effective in terms of response rates and time to therapy compared with other drugs like Tamoxifen [18].

Breast cancer is the most common invasive cancer in women. The use of letrozole, which blocks estrogen synthesis, is an excellent therapy for postmenopausal women with hormone-dependent breast cancer [19]. Estrogen is recognized as a major risk factor in most breast cancers. Thus, the use of most potent inhibitors of aromatase appears to be a reasonable strategy. Many studies have introduced letrozole as the most powerful of the third-generation inhibitors of aromatase [20].

In this research AgNPs were synthesized by a biosynthetic method using olive leaf extracts and its surface modified by cysteine as an appropriate ligand. We conducted loading experiments under varying conditions and determined the adsorption efficiency using UV spectroscopy. Moreover, we plotted and fitted sorption isotherms of linear and non-linear to the models of Langmuir, Freundlich, Dubinin-Radushkevich and Temkin. Sorption kinetics data of linear and non-linear were fitted to the models of pseudo-first-order, pseudo-second-order and intra particle diffusion model. Finally, the drug release of the letrozole loaded Cys-AgNPs was investigated in simulated gastric and intestinal fluid buffer in vitro.

2. Experimental

2-1. Instruments

UV-Vis spectrum analysis was done by using a UV-Vis spectrophotometer (Cary 300, Agilent, USA). High-resolution TEM images were obtained using the Philips, EM, 208 Manufacture Specification model (Netherlands), and infrared spectra were recorded on a Thermo Nicolet Nexus 870, (USA) Fourier transform infrared spectrometer. Elemental analysis was carried out on a CHN Analyzer Euro EA300 model (Milan, Italy).

2-2. Reagents and solutions

Silver nitrate and cysteine were purchased from Merck (Darmstadt, Germany). Live leaves were taken from the olive research institute, Roodbar, Iran. Letrozole drug was purchased from Sigma-Aldrich. The stock solutions (500 and 50 ppm) of letrozole, were prepared by dissolving appropriate amounts of letrozole in methanol. 0.01 M acetic acid - acetate buffer (pH 3–6.5) or 0.01 M phosphate buffer (pH 6.5–8) were used wherever needed to adjust the pH of the solution. Distilled water was used in the preparation of buffers and standard solution.

2-3. Preparation of olive extract

Fresh olive leaves were surface cleaned with running tap water, followed by distilled water and dried at room temperature. 5 g plant leaf powder was boiled with 250 mL of distilled water at 100 °C for 20 min. After filtering (Whatman No: 3), clear leaf extract was stored at 4 °C for further use.

2-4. Synthesis and Characterization of AgNPs

To synthesize AgNPs, 20 mL of olive leaf extract was added into 80 mL of aqueous solution of 1 mM silver nitrate and stored in the dark condition overnight at room temperature. The color change from light yellow to dark brown (Fig. 1), indicated the successful formation of AgNPs. The obtained solution was centrifuged at 14,000 rpm for 15 min, washed two times with distilled water, dried at room temperature and collected. UV-visible spectrum analysis was done after diluting a small amount of the sample into deionized water in a wavelength range between 350 and 700 nm. Deionized water was used as a reference [21]. TEM was used to reveal the size and morphology of the AgNPs.

2-5. Surface Modification of AgNPs with Cysteine (Cys-AgNPs)

Amino acid cysteine was chosen as an appropriate ligand to improve the surface structure of nanoparticles. Covering of the AgNPs with cysteine causes the stability of nanoparticles via a hydrogen bond between the amino acid and the nanoparticle surface. A solution of 0.5% cysteine was prepared using distilled water and 20 cc of this solution was mixed with 0.01 g AgNPs for two hours in the dark under vigorous stirring condition (90 rpm). The produced nano-sorbent was centrifuged and dried at room temperature for 24 hours. To confirm the formation of Cys-AgNPs, the spectrum of the cysteine and produced nano-sorbent was recorded by FTIR spectrophotometer. Also Cys-AgNPs was tested to measure carbon (C), hydrogen (H) and nitrogen (N) using CHN analyzer.

2-6. Determination of wavelength of maximum absorbance (λ_{max})

The adsorption curve of several concentration of letrozole was obtained using a spectrophotometer. Then, at the λ_{max}, adsorption of the remaining concentrations of letrozole was read and the adsorption graph of different concentrations was drawn.

2-7. Determination of optimum pH

10 mL of letrozole solution (20 ppm) containing 2.5 mL of buffers with pH 3, 4, 5,6,7,8,9,10 was prepared. Then, 15 mL of each solutions was mixed with 0.005 g of nano-adsorbent. Samples were placed on the shaker and then centrifuged and the supernatant solution was evaluated by a spectrophotometer. For evaluation the optimal pH,

absorbance of samples at each pH and standard as well was separately examined. The optimum pH was determined using the following equation:

$$Q = \frac{C_0 - C_e \times V}{W} \quad (1)$$

C_0 and C_e (mg L^{-1}) are primary and equilibrium concentrations of the letrozole, respectively, V (L) is the volume of the solution, and W (*g*) is the mass of the Cys-AgNPs.

2-8. Isotherm studies

The association between adsorbate amount on adsorbent and equilibrium concentrations of adsorbate in the solution can be explained by adsorption isotherm, indicating the diffusion manner of adsorbate molecules between liquid and solid phases when the process of adsorption is close to equilibrium [22]. The results concerning the adsorption of letrozole on Cys-AgNPs are aligned with those reported by Langmuir, Freundlich, Temkin and Dubinin- Radushkevich (D-R) for adsorption isotherm.

The Langmuir model considers that the ideal monolayer adsorption takes place at specific identical active sites [23].

The Langmuir isotherm model (Eq. 2) and its nonlinear form (Eq. 3) can be expressed as follows:

$$C_e/q_e = 1/K_l q_{max} + C_e/q_{max} \quad (2)$$

$$q_e = q_{max} K_L C_e/(1 + K_L C_e) \quad (3)$$

where, q_{max} denotes the maximum valence of letrozole sorption resembling thorough monolayer coverage on the Cys-AgNPs surface (mg g^{-1}), and K_L indicates the Langmuir constant (Lmg^{-1}). C_e is the equilibrium concentration of letrozole (mg L^{-1}), q_e is the adsorption capacity at equilibrium (mg g^{-1}), the fundamental characteristics of the Langmuir equation is represented in terms of a dimensionless separation factor, R_L, described as:

$$R_L = 1/1 + K_L C_0 \quad (4)$$

Studies have shown [24] that R_L values indicate the adsorption to be irreversible ($R_L = 0$), desirable ($0 < R_L < 1$), linear ($R_L = 1$), or undesirable ($R_L = 1$).

We used the Freundlich isotherm to characterize heterogeneous systems, where it was measured by the heterogeneity factor 1/n. The Freundlich isotherm model (Eq. 5) and its nonlinear form (Eq. 6) are presented by the following equations:

$$Ln\ q_e = 1/n \ln C_e + \ln k_f \quad (5)$$

$$q_e = K_f C_e^{1/n} \quad (6)$$

where, K_F indicates the Freundlich constant ($L \cdot mg^{-1}$) [25].

According to the Temkin isotherm equation, the sorption heat of all molecules in the layer drops with coverage in a linear manner due to Cys-AgNPs interactions [26], the Temkin isotherm model (Eq. 7) and its nonlinear form (Eq. 8) are given by the following equations:

$$q_e = B \ln A + B \ln C_e \quad (7)$$

$$qe = B \ln (ACe) \quad (8)$$

where constant $B = RT/b$ is related to the heat of letrozole sorption (J mol^{-1}), R the universal gas constant (8.314 J $mol^{-1}K^{-1}$) and T is the temperature (*K*). A is the constant of equilibrium binding (L g^{-1}).

Dubinin-Radushkevich (D-R) isotherm model is an experimental sorption model used to express the sorption mechanism with Gaussian energy distribution on heterogeneous surfaces [27]. The D-R isotherm model (Eq. 9) and its nonlinear form (Eq. 10) are presented by the following equations:

$$\ln q_e = \ln q_s - D\varepsilon^2 \quad (9)$$

$$q_e = (q_D) \exp - D\varepsilon^2 \quad (10)$$

$$\varepsilon = RT \ln (1+1/C_0) \quad (11)$$

where, D ($mol^2\ kJ^{-2}$) indicates D-R constant. The value of ε represents the Polanyi potential.

2-9. Sorption Kinetics

For the description of kinetic data, we used three sorption kinetic models: pseudo-first-order (PFO), pseudo-second-order (PSO) and intra-particle diffusion (IPD) models. The PFO kinetic model is based on the assumption that the rate of change of solute uptake with time is directly proportional to the difference in saturation concentration and the amount of solid uptake with time, which is generally applicable over the initial step of an adsorption method. The PSO model is based on the assumption that the rate-limiting stage is chemisorption or chemical sorption and predicts the behavior over the whole range of sorption. To identify the diffusion mechanism in the adsorption, intraparticle mass transfer diffusion model (IPD) has been proposed by Weber and Morris. This step occurs via two mechanisms: pore diffusion and surface diffusion. Particle porosity (morphology, distribution) and tortuosity are key agents affecting the pore diffusion [28].

The PFO model is as follows:

$$\ln (q_e - q_t) = \ln q_e - k_1 t \quad (12)$$

On the other hand, the nonlinear form of PFO kinetic as follows:

$$q_t = q_e (1 - e^{-k1.t}) \quad (13)$$

The PSO model is expressed in the following equation:

$$t/q_t = 1/k_2 q_e^2 + t/q_e \quad (14)$$

Also, the nonlinear form of PSO kinetic is as follows:

$$q_t = (k_2 q e^2 \cdot t)/(1+k_2\, q_e \cdot t) \quad (15)$$

where, q_t (mg g^{-1}) denotes the amount of drug adsorption on the adsorbent at time (min). The rate constants of the PFO and the PSO are also shown by K_1 (min^{-1}) and K_2 (g mg^{-1} min^{-1}), respectively.

IPD model is described as follows:

$$q_t = k_i t^{1/2} + C \quad (16)$$

where, K_i (mg g^{-1} $min^{-1/2}$) indicates the rate constant of IPD, and c is the constant of model.

2-10. In vitro drug release

Letrozole release study was determined by measuring the absorbance peak at 240 nm. To this purpose, letrozole loaded Cys-AgNPs was transferred to the dialysis bag and put in to simulate gastric fluid buffer, pH 1.2 in a shaker incubator 37 °C for 30 min. Subsequently, the dialysis bags were transferred to simulated intestinal fluid buffer, pH 7.4 for 30 hours. Samples were withdrawn at specified time intervals and replaced with fresh medium and assayed by a UV spectrophotometer. All experiments were performed in triplicate. Then the cumulative amount of drug released at time $t(q_t)$ was reported.

3. Results and Discussion

3-1. Adsorbent characteristics

This study was focused on the investigation of adsorption and release behavior of letrozole-loaded biosynthesized and cysteine-capped AgNPs optimization conditions to develop a highly loaded and released formulation. For this purpose, nanoparticles were biosynthesized and characterized by determining the average particle diameter using TEM. The presence of cysteine on nanoparticles surface was verified by CHN analysis and FT-IR.

3-1-1. Characterization of synthesized AgNPs

The solution changed from yellow to dark brown, which indicated that the AgNPs were yielded at 24 h (Fig. 1). The synthesis of AgNPs by Aloe-vera extract after 24 h incubation was conducted by Chandran *et al*. [29].

Fig. 2 displays the AgNPs UV–visible spectra using olive leaf extract at ambient temperature after 24 h. The results show maximum absorbance at 430 nm, which indicates the presence of AgNPs (Fig. 2). Ahmad *et al*. saw the same peak during their studied on green synthesis of AgNPs using extracts of Ananascomosus in 2012 [30].

The scanning of AgNPs synthesized by olive leaf extract was performed by TEM (Philips, EM, 208). The results reveal that the mean size of AgNPs is spherical and in the range of 10 to 50 nm, as illustrated in Fig. 3.

3-1-2. Characterization of Cys-AgNPs

AgNPs surface modifications were confirmed using FTIR. The FTIR spectrum of free cysteine indicated the band at 1125 cm^{-1} assigned to C-O, the peak at 1335 cm^{-1} was due to COO, the peak at 1581 cm^{-1} can be due to NH and the peak at 1484 cm^{-1} was due to CH_2. We did not observe the free cysteine's S-H vibrational band at 2584 cm^{-1} within the spectra of the isolated Cys-AgNPs powder.

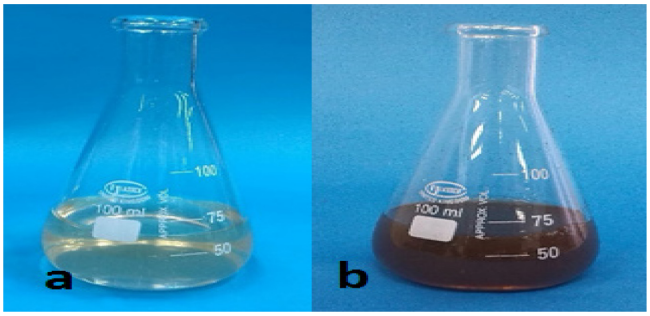

Fig. 1. Impact of $AgNO_3$ on olive leaf extracts (a) before and (b) after adding the $AgNO_3$; the color change of the reaction mixture is also shown.

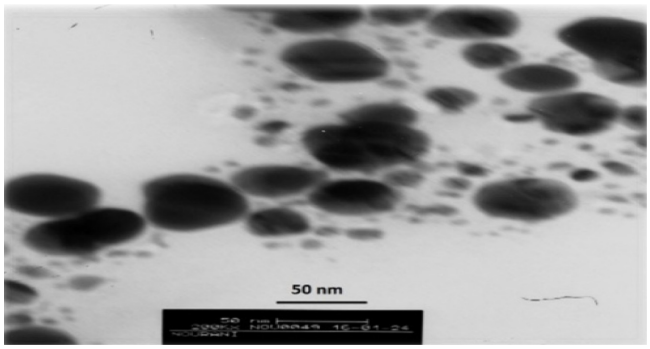

Fig. 3. TEM image of AgNPs synthesized using olive leaf extract, showing the spherical shaped particle size ranges from 10 to 50 nm.

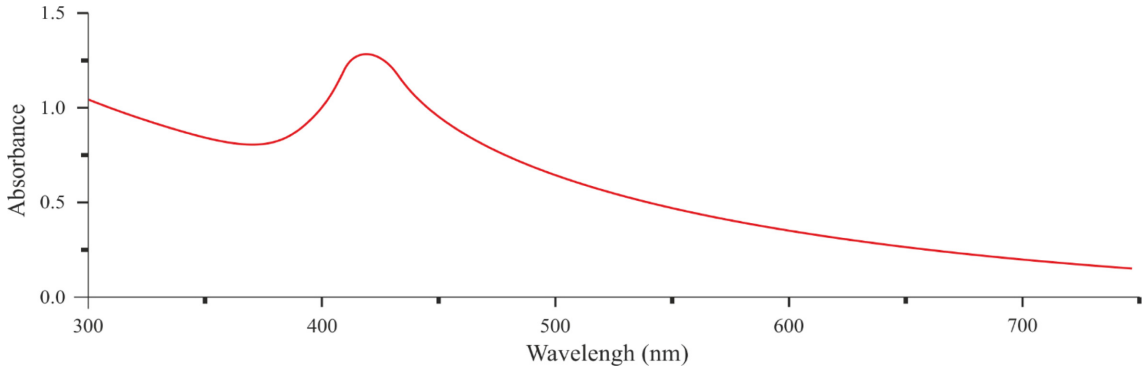

Fig. 2. UV-Vis adsorption spectrum of AgNPs synthesized by exposure of olive leaf extract broth with 1 mM silver nitrate.

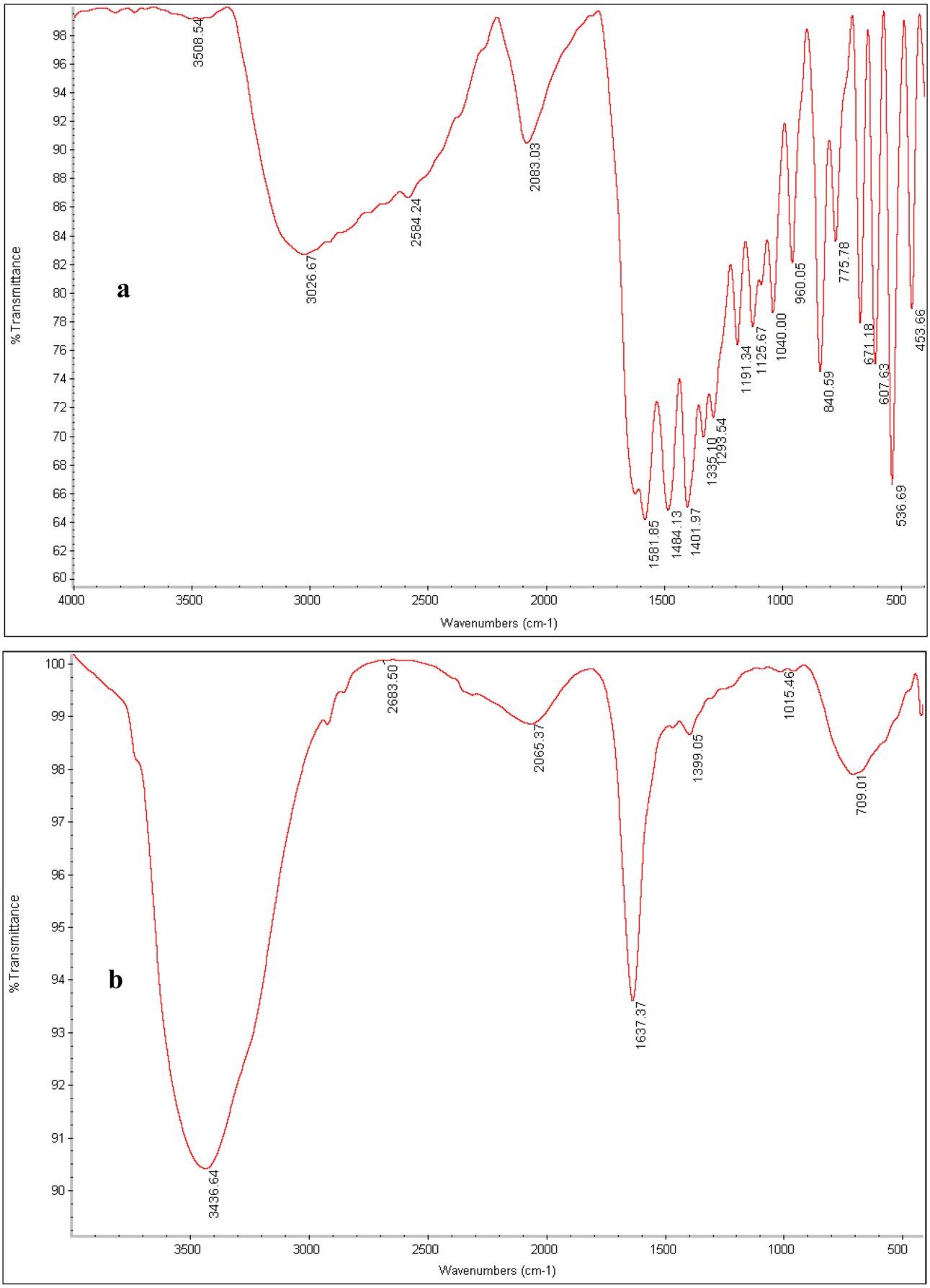

Fig. 4. FTIR spectra of (a) free amino acid cysteine (b) cysteine capped AgNPs.

This provides strong evidence of cysteine surface binding to the silver particles through a thiolate linkage. A similar behavior on the modification of alkane thiol by gold nanoparticles was investigated by Templeton *et al*. [31]. Further indication for the existence of cysteine on the surface of AgNPs after modification procedure was prepared by FTIR spectrum of the Cys-AgNPs in which carboxylate stretch vibration of the cysteine molecules was observed at 1637 cm^{-1}. The peak at 3436 cm^{-1} was assigned to OH groups (Fig. 4).

To confirm the formation of Cys-AgNPs, CHN analysis test was performed. The results indicate the presence of carbon (0.99%), hydrogen (0.97%) and nitrogen (8.34%) in the sample, while free AgNPs does not contain these elements. On the other hand, in Cys-AgNPs, due to the modification of AgNPs surface with Cys, the value of nitrogen was increased.

3-2. Optimization of parameters

We examined letrozole sorption at different pH (3–10) by the batch method. According to the experimental results shown in Fig. 5, best sorption was obtained at pH 8. This can be attributed to carboxylic acidic groups' elevated protonation on Cys-AgNPs surface and the consequent strengthening of hydrogen bonding with nitrogen atoms in letrozole. The protonation diminishes with the rise of pH, leading to the dominance of electrostatic repulsive power. As can be seen in Fig. 5, Q (mg g^{-1}) is the adsorption capacity of adsorbent. Therefore, the maximum adsorption capacity was 34.56 mg g^{-1}.

3-3. Adsorption isotherms

Isotherm studies were performed by adding a fixed amount of nano-adsorbent (0.01 g) to a series of tubes filled with 10 mL diluted solutions of letrozol (2-60 mg L^{-1}). After shaking for 20 min, the tubes were centrifuged. The supernatant phase was separated and the amount of drug was estimated at a maximum adsorption wavelength (λ_{max}) by UV-Vis spectrophotometry. The linear and nonlinear forms of Langmuir, Freundlich, Temkin and Dubinin-Radushkevich (D-R) models were compared to get the best isotherm model. As can be seen from Table 1, the Langmuir isotherm has the highest regression coefficients for both linear (0.998) and non-linear (0.999). According to the values obtained by Langmuir isotherm, the values of R_L for linear and non-linear methods was 0.353 and 0.343, respectively. Calculating the R_L value demonstrated desirable adsorption (0< RL<1) for letrozole. The Freundlich constant (n) was 1.272 and 1.575 for linear and non-linear methods, respectively; that was expressive of the desirability of adsorption process [32]. Fig. 6 presents the non-linear isotherm models for letrozole adsorption by Cys-AgNPs at 25 °C.

3-4. Sorption Kinetics

The batch technique was used to investigate the % sorption of letrozole onto the synthesized adsorbent at optimum contact time. A set of solutions containing 20 ppm letrozole was taken in a micro test tube and their pH were adjusted to the optimum value. Cys-AgNPs

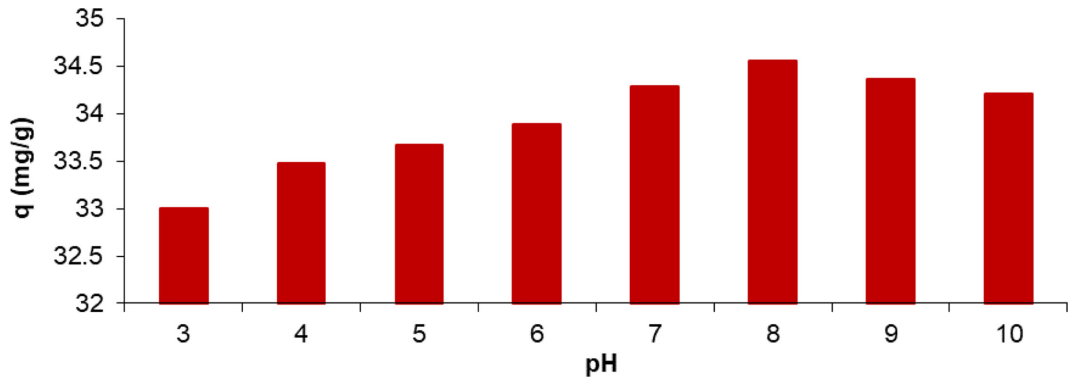

Fig. 5. Influence of initial pH on the adsorption of letrozole on Cys-AgNPs.

Table 1. Isotherm parameters obtained by using linear and non-linear method at 25 °C

		q_{max} (mg g^{-1})	k_l (L mg^{-1})	R_L	R^2
Langmuir	Linear	49.751	0.030	0.353	0.998
	Non-linear	48.665	0.031	0.343	0.999
		k_f (L mg^{-1})	n		R^2
Freundlich	Linear	1.692	1.272		0.987
	Non-linear	2.657	1.575		0.990
		q_m (mg g^{-1})	B		R^2
Dubinin-Radushkevich	Linear	15.743	1.058		0.757
	Non-linear	25.722	12.241		0.924
		A (L g^{-1})	B		R^2
Temkin	Linear	0.327	10.403		0.992
	Non-linear	0.687	7.515		0.942

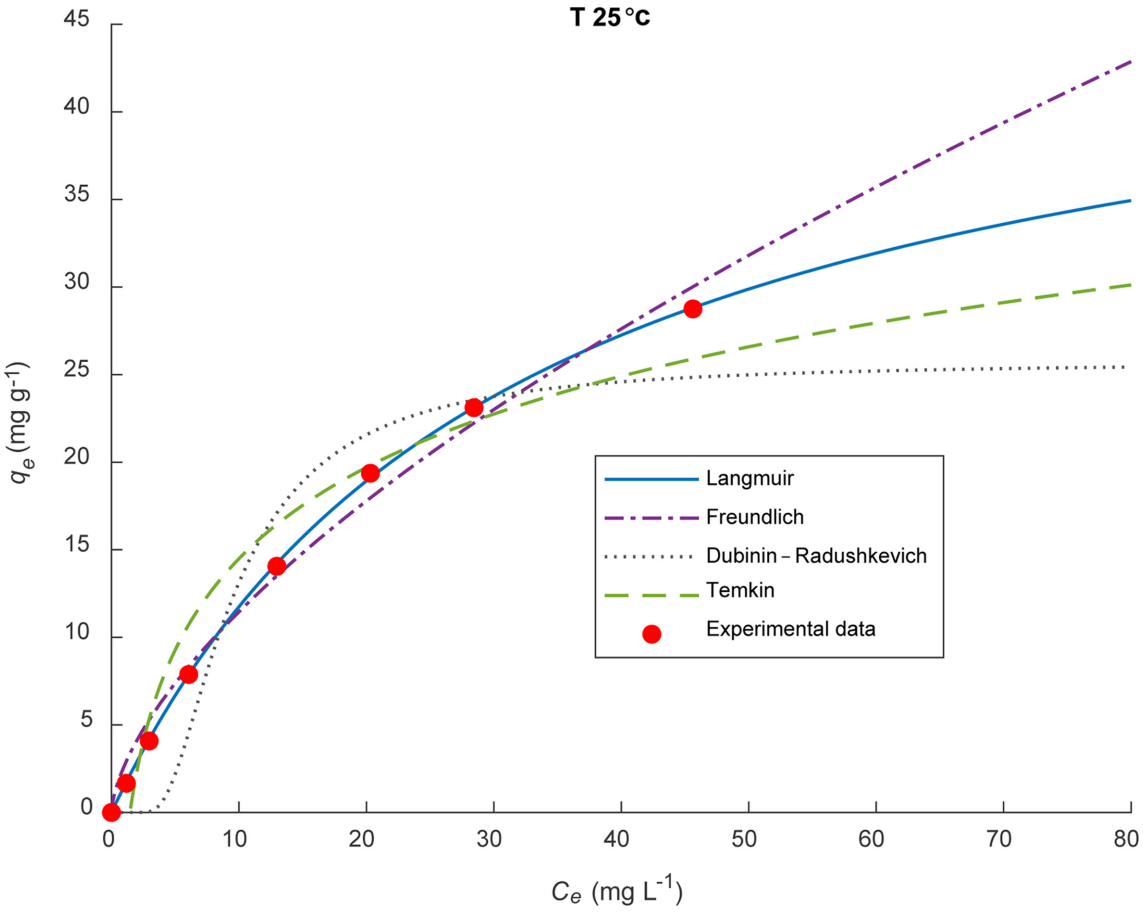

Fig. 6. Non-linear isotherm model for letrozole adsorption onto Cys-AgNPs.

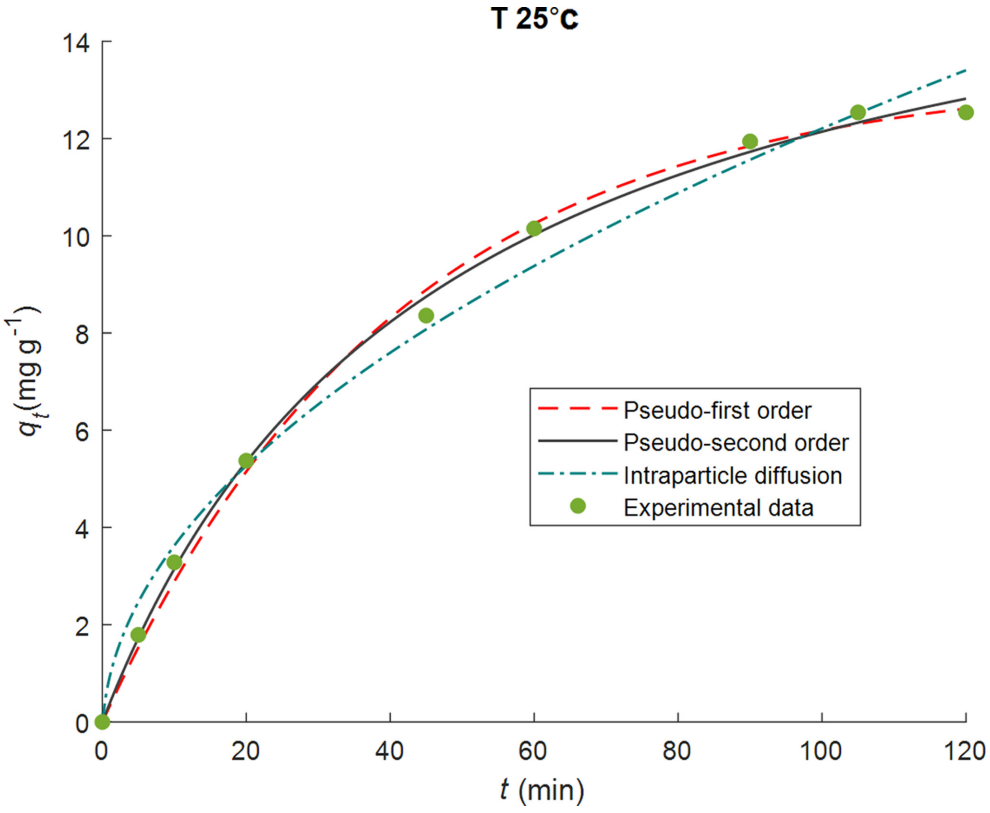

Fig. 7. Non-linear kinetic model for letrozole adsorption onto Cys-AgNPs.

(0.05 g) was added to each solution. The samples were shaken for different periods of time (0, 5, 10, 20, 45, 60, 90, 105, 120 min), then compared in terms of absorbance with each other and with standard absorbance.

As the results indicate, the synthesized Cys-AgNPs exhibit the highest adsorption for letrozole during the first one min because of the available active sites on adsorbent and subsequently, with increasing time, the adsorption rate has a stable trend. Therefore, the process of adsorption does not require a long contact time. It can also be concluded that sites on the synthesized Cys-AgNPs are available for the drug.

The pseudo-first-order (PFO), pseudo-second-order (PSO) and the intraparticle diffusion (IPD) kinetic models were investigated using linear and non-linear regression methods. The lines in the plot of q_t vs. t presented good agreement of the experimental data with the PSO kinetic model for letrozole adsorption onto Cys-AgNPs (Fig. 7). The kinetics constants and correlation coefficient (R^2) are presented in Table 2. The results show that the PSO kinetic was the best model for the letrozole adsorption on Cys-AgNPs with R^2 of 0.996 and 0.998 for linear and non-linear methods, respectively.

3-5. Letrozole release

The release of letrozole by Cys-AgNPs in simulated intestinal and gastric fluid is shown in Fig. 8. Approximately, 40% of the letrozole was released in the simulated intestinal fluid over a period of 30 min at 37 °C and then the amount of drug remaining was released in the intestinal fluid with a relatively gentle gradient for 10 hours.

Mondal et al. studied the letrozole release from poly (D,L-lactide-co-glycolide (PLGA) nanoparticles. The release profiles show about 45–69% of drug was released up to more than 24 h. Therefore, the entire drug loaded on PLGA nanoparticles could not be released [33]. Kumar Dey et al. studied letrozole loaded biodegradable nanoparticles for breast cancer therapy. They investigated the release of drug within 15 hours and only less than 20% of the drug was released [34]. In this study, the entire drug loaded on modified AgNPs was successfully released with a slow release time of 10 hours.

4. Conclusions

This study has introduced the novel cysteine capped AgNPs for high letrozole adsorption and release levels. The results illustrate that the proposed biosynthesized nanoparticles offer multiple advantages, including cost-effectiveness and environmental friendliness compared to physico-chemical methods. In this study, the non-linear isotherm model hasd better performance, compared with a linear isotherm. The results indicated that the non-linear Langmuir isotherm is a more suitable model ($R^2 = 0.999$) for describing the adsorption of letrozole onto Cys-AgNPs. The parameters of R_L (0.343) and n

Table 2. Kinetic parameters obtained by using linear and non-linear method at 25 °C

		q_e (mg g^{-1})	k_1 (min^{-1})	R^2
Pseudo-first-order	Linear	11.975	0.029	0.984
	Non-linear	13.324	0.024	0.996
		q_e (mg g^{-1})	k_2 (g mg^{-1} min^{-1})	R^2
Pseudo-second-order	Linear	17.543	0.0012	0.996
	Non-linear	17.786	0.0012	0.998
		K_i (mg g^{-1} min$^{-1/2}$)	c	R^2
Intraparticle diffusion	Linear	-	-	-
	Non-linear	1.254	0.339	0.988

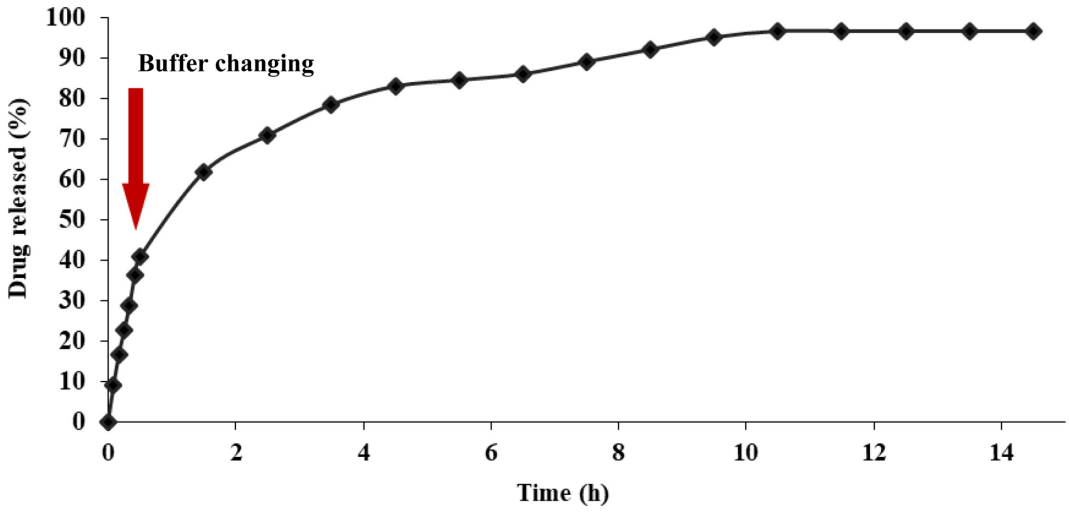

Fig. 8. The releasing of letrozole by Cys-AgNPs.

(1.575) indicated that the letrozole sorption rate on Cys-AgNPs is favorable. The results showed that the non-linear pseudo-second-order kinetic ($R^2 = 0.998$) is a more suitable model for describing the adsorption of letrozole onto Cys-AgNPs. The in vitro release profile indicates about 100% of letrozole was released in conditions of the human body after 10 h. Thus, Cysteine capped silver nanoparticles can be a good candidate for carrying and releasing letrozole as a novel drug delivery system for breast cancer therapy.

Acknowledgments

The results described in this paper were part of student thesis. The authors thank all laboratory staff of Islamic Azad University, Science and Researches Branch.

The authors declare no conflict of interest.

References

1. Sriharitha, P. J. and Swaroop, H., "A Review on Nanoparticles in Targeted Drug Delivery System, Research & Reviews," *Journal of Material Science*, **4**, 1-6(2006).
2. Yang, H.-W., Hua, M.-Y., Liu, H.-L., Huang, C.-Y. and Wei, K.-C., "Potential of Magnetic Nanoparticles for Targeted Drug Delivery," *Nanotechnology, Science and Applications*, **5**, 73(2012).
3. Jayapriya, E. and Lalitha, P., "Synthesis of Silver Nanoparticles Using Leaf Aqueous Extract of Ocimum Basilicum (L.)," *International Journal of ChemTech Research*, **5**, 2985-2992(2013).
4. Thakare, S. R. and Ramteke, S. M., "Fast and Regenerative Photocatalyst Material for the Disinfection of *E. coli* from Water: Silver Nano Particle Anchor on MOF-5," *Catalysis Communications*, **102**, 21-25(2017).
5. Prusty, K. and Swain, S. K., "Nano Silver Decorated Polyacrylamide/dextran Nanohydrogels Hybrid Composites for Drug Delivery Applications," *Materials Science and Engineering C*, **85**, 130-141(2017).
6. Li, L., *et al*., "Effect of Stable Antimicrobial Nano-silver Packaging on Inhibiting Mildew and in Storage of Rice," *Food Chemistry*, **215**, 477-482(2017).
7. Juling, S., *et al*., "*In vivo* Distribution of Nanosilver in the Rat: The Role of Ions and de Novo-formed Secondary Particles," *Food Chem Toxicol*, **97**, 327-335(2016).
8. Wilding, L. A., *et al*., "Repeated Dose (28-day) Administration of Silver Nanoparticles of Varied Size and Coating Does Not Significantly Alter the Indigenous Murine Gut Microbiome," *Nanotoxicology*, **10**, 513-520(2016).
9. Bergin, I. L., *et al*., "Effects of Particle Size and Coating on Toxicologic Parameters, Fecal Elimination Kinetics and Tissue Distribution of Acutely Ingested Silver Nanoparticles in a Mouse Model," *Nanotoxicology*, **10**, 352-360(2016).
10. Shahare, B. and Yashpal, M., "Toxic Effects of Repeated Oral Exposure of Silver Nanoparticles on Small Intestine Mucosa of Mice," *Toxicol Mech Methods*, **23**, 161-167(2013).
11. Prabhu, S. and Poulose, E. K., "Silver Nanoparticles: Mechanism of Antimicrobial Action, Synthesis, Medical Applications, and Toxicity Effects," *International Nano Letters*, **2**, 32(2012).
12. Shanmugavadivu, M., Kuppusamy, S. and Ranjithkumar, R., "Synthesis of Pomegranate Peel Extract Mediated Silver Nanoparticles and Its Antibacterial Activity," *Am. J. Adv. Drug. Deliv*, **2**, 174-182(2014).
13. Khalil, M. M., Ismail, E. H., El-Baghdady, K. Z., Mohamed, D., "Green Synthesis of Silver Nanoparticles Using Olive Leaf Extract and its Antibacterial Activity," *Arabian Journal of Chemistry*, **7**, 1131-1139(2014).
14. Cho, K., Wang, X., Nie, S. and Shin, D. M., "Therapeutic Nanoparticles for Drug Delivery in Cancer," *Clinical Cancer Research*, **14**, 1310-1316(2008).
15. Gong, R. and Chen, G., "Preparation and Application of Functionalized Nano Drug Carriers," *Saudi Pharmaceutical Journal*, **24**, 254-257(2016).
16. Sperling, R. A. and Parak, W. J., "Surface Modification, Functionalization and Bioconjugation of Colloidal Inorganic Nanoparticles, Philosophical Transactions of the Royal Society A: Mathematical," *Physical and Engineering Sciences*, **368**, 1333-1383(2010).
17. Barzegar-Jalali, M., Adibkia, K., Valizadeh, H., Shadbad, M. R. S., Nokhodchi, A., Omidi, Y., Mohammadi, G., Nezhadi, S. H. and Hasan, M., "Kinetic Analysis of Drug Release from Nanoparticles," *Journal of Pharmacy and Pharmaceutical Sciences*, **11**, 167-177(2008).
18. Panahi, H. A., Nezhati, M. N., Kashkoieh, R. A., Moniri, E., Galaev, I. Y., "Poly[1-(N,N-bis-carboxymethyl) amino-3-allylglycerol-co-dimethylacrylamide] Brushes Grafted Onto Siliceous Support for Preconcentration and Determination of Cobalt (II) in Human Plasma and Environmental Samples," *Korean Journal of Chemical Engineering*, **30**, 1722-1728(2013).
19. Geisler, J., Helle, H., Ekse, D., Duong, N. K., Evans, D. B., Nordbø, Y., Aas, T. and Lønning, P. E., "Letrozole is Superior to Anastrozole in Suppressing Breast Cancer Tissue and Plasma Estrogen Levels," *Clinical Cancer Research*, **14**, 6330-6335(2008).
20. Bhatnagar, A. S., "The Discovery and Mechanism of Action of Letrozole," *Breast Cancer Research and Treatment*, **105**, 7-17 (2007).
21. Kalaki, Z. A., Safaeijavan, R., Ortakand, M. M., "Biosynthesis of Silver Nanoparticles Using Mentha longifolia (L.) Hudson Leaf Extract and Study its Antibacterial Activity," *Archives of Advances in Biosciences*, **8**, 24-30(2017).
22. Freitas, A., Mendes, M. and Coelho, G., "Thermodynamic Study of Fatty Acids Adsorption on Different Adsorbents," *The Journal of Chemical Thermodynamics*, **39**, 1027-1037(2007).
23. Langmuir, I., "The Adsorption of Gases on Plane Surfaces of Glass, Mica and Platinum," *Journal of the American Chemical Society*, **40**, 1361-1403(1918).
24. Hall, K. R., Eagleton, L. C., Acrivos, A. and Vermeulen, T., "Pore-and Solid-diffusion Kinetics in Fixed-bed Adsorption Under Constant-pattern Conditions," *Industrial & Engineering Chemistry Fundamentals*, **5**, 212-223(1966).
25. Hashemian, S., Ardakani, M. K. and Salehifar, H., "Kinetics and Thermodynamics of Adsorption Methylene Blue Onto Tea Waste/$CuFe_2O_4$ Composite(2013).
26. Thabet, M. S. and Ismaiel, A. M., "Sol-Gel γ-Al_2O_3 Nanoparticles Assessment of the Removal of Eosin Yellow Using: Adsorption, Kinetic and Thermodynamic Parameters," *Journal of Encapsulation and Adsorption Sciences*, **6**, 70(2016).

27. Ayawei, N., Ekubo, A., Wankasi, D. and Dikio, E., "Adsorption of Congo Red by Ni/Al-CO_3: Equilibrium, Thermodynamic and Kinetic Studies," *Oriental Journal of Chemistry*, **31**, 1307-1318 (2015).
28. Ranjan Sahoo, T. and Prelot, B., "Chapter 7 - Adsorption Processes for the Removal of Contaminants from Wastewater: the Perspective Role of Nanomaterials and Nanotechnology," *Nanomaterials for the Detection and Removal of Wastewater Pollutants*, 161-222(2020).
29. Chandran, S. P., Chaudhary, M., Pasricha, R., Ahmad, A. and Sastry, M., "Synthesis of Gold Nanotriangles and Silver Nanoparticles Using Aloevera Plant Extract," *Biotechnology Progress*, **22**, 577-583(2006).
30. Ahmad, N. and Sharma, S., Green synthesis of silver nanoparticles using extracts of Ananas comosus(2012).
31. Templeton, A. C., Chen, S., Gross, S. M. and R.W. Murray, "Water-soluble, Isolable Gold Clusters Protected by Tiopronin and Coenzyme A Monolayers," *Langmuir*, **15**, 66-76(1999).
32. Konicki, W., Aleksandrzak, M., Moszyński, D., Mijowska, E., "Adsorption of Anionic Azo-dyes from Aqueous Solutions Onto Graphene Oxide: Equilibrium, Kinetic and Thermodynamic Studies," *Journal of Colloid and Interface Science*, **496**, 188-200(2017).
33. Mondal, N., Pal, T. and Ghosal, S., "Development, Physical Characterization, Micromeritics and in vitro Release Kinetics of Letrozole Loaded Biodegradable Nanoparticles," *Die Pharmazie-An International Journal of Pharmaceutical Sciences*, **63**, 361-365(2008).
34. Dey, S. K., Mandal, B., Bhowmik, M. and Ghosh, L. K., "Development and in vitro Evaluation of Letrozole Loaded Biodegradable Nanoparticles for Breast Cancer Therapy," *Brazilian Journal of Pharmaceutical Sciences*, **45**, 585-591(2009).